ORNL/SPR-2024/14

Decarbonizing Cooking Appliances with Hydrogen

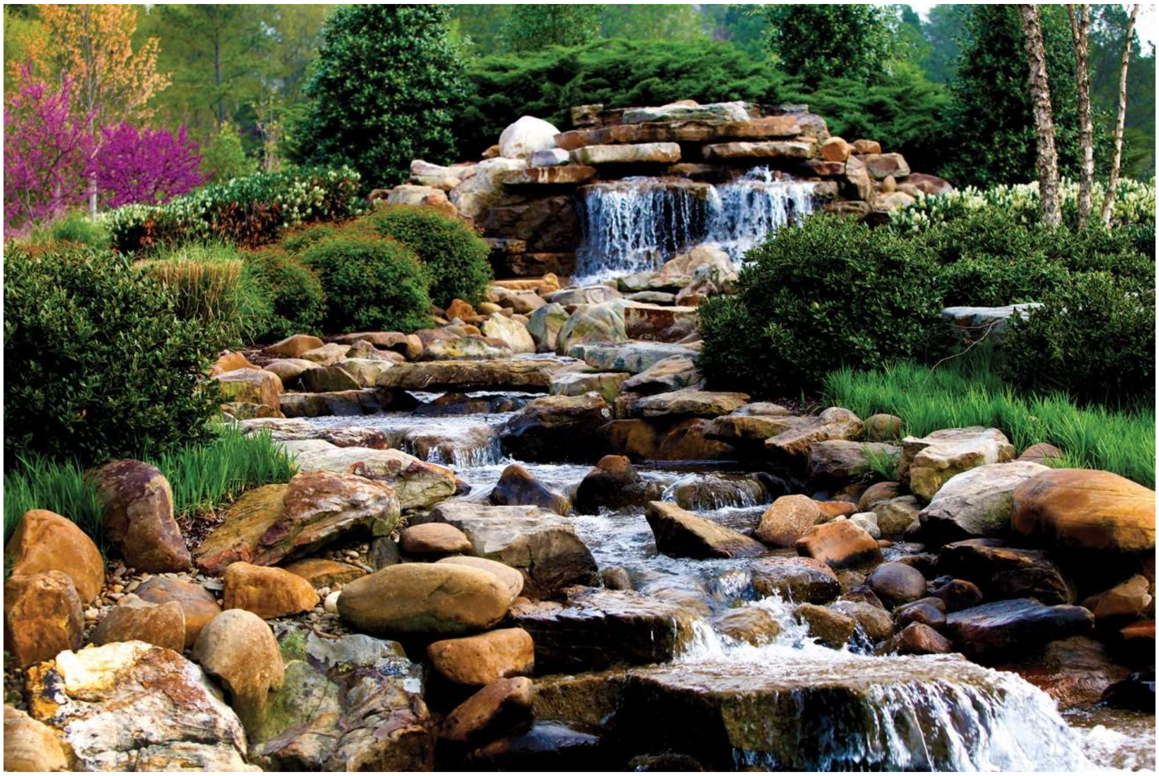

Praveen Cheekatamarla

March 2024

DOCUMENT AVAILABILITY

Online Access: US Department of Energy (DOE) reports produced after 1991 and a growing number of pre-1991 documents are available free via https://www.osti.gov.

The public may also search the National Technical Information Service's National Technical Reports Library (NTRL) for reports not available in digital format.

DOE and DOE contractors should contact DOE's Office of Scientific and Technical Information (OSTI) for reports not currently available in digital format:

US Department of Energy
Office of Scientific and Technical Information
PO Box 62
Oak Ridge, TN 37831-0062
Telephone: (865) 576-8401
Fax: (865) 576-5728
Email: reports@osti.gov
Website: www.osti.gov

ORNL/SPR-2024/14

Buildings and Transportation Science Division

DECARBONIZING COOKING APPLIANCES WITH HYDROGEN

Praveen Cheekatamarla

March 2024

Prepared by
OAK RIDGE NATIONAL LABORATORY
Oak Ridge, TN 37831
managed by
UT-BATTELLE LLC
for the
US DEPARTMENT OF ENERGY
under contract DE-AC05-00OR22725

CONTENTS

LIST OF FIGURES

ABBREVIATIONS

HHV	higher heating value
IR	infrared
LHV	lower heating value
NG	natural gas
NOx	nitrogen oxide
ORNL	Oak Ridge National Laboratory
RV	recreational vehicle
WC	water column

EXECUTIVE SUMMARY

This project is a collaboration between the US Department of Energy's Oak Ridge National Laboratory and Southern California Gas Company. The primary objective of this cooperative research and development agreement is to develop a clean, safe cooking appliance capable of operating on hydrogen and natural gas (NG) fuels.

Combustion system design and burner configuration play vital roles in the overall performance of any heating system. Energy conversion efficiency, emissions, reliability, safety, and longevity rely on the efficacy of the combustion process. The high flame velocity and temperature of hydrogen fueled burners also make them susceptible to flashback and higher nitrogen oxide (NO_x) emissions.

Considering all these risk and performance factors, a novel hydrogen-compatible heterogeneous burner prototype was engineered, fabricated, and evaluated for applications in cooking appliances. The key features targeted and accomplished under this effort included fuel flexibility, tolerance to high hydrogen concentrations (up to 85% in atmospheric design and 100% in premixed design), a wide range of thermal power ratings, thermal cycling, reliability, and most importantly, safety. The burner was operated in the range of 3,000–10,000 Btu/h while supplied with hydrogen at different concentrations under all practical operating conditions (cold start, hot restart, fuel concentration variance). The heterogeneous oxidation burner technology was evaluated for overall performance targeting safety, reliability, emissions, fuel flexibility, and energy efficiency in commercial recreational vehicle (RV) and residential cooking range appliance prototypes. The burner demonstrated safe, reliable performance generating infrared (IR) heating energy without consuming parasitic energy while using low-cost materials. Performance evaluation testing of the novel IR burner demonstrated fuel flexibility with hydrogen-blended natural gas while eliminating air pollutants like NO_x and methane and increasing energy efficiency by up to 20%.

1. BURNER DESIGN AND DEVELOPMENT

1.1 TEST SETUP AND BURNER DESIGN

The primary objective of this preliminary work was to develop a cooking appliance burner capable of accepting a wide range of hydrogen-blended natural gas compositions while operating in a safe manner. The test facility to evaluate hydrogen blends of natural gas in a cooking appliance burner was commissioned. The primary components of the test facility include: (i) air–fuel metering and mixing, (ii) gas shut-off valve, (iii) burner module and heat containment, (iv) combustion product's temperature control, (v) heat exchanger with integrated liquid coolant, and (vi) data acquisition. Fuel metering was accomplished via mass flow meters (Azbil model CMS0050). Figure 1 show a picture of the test facility.

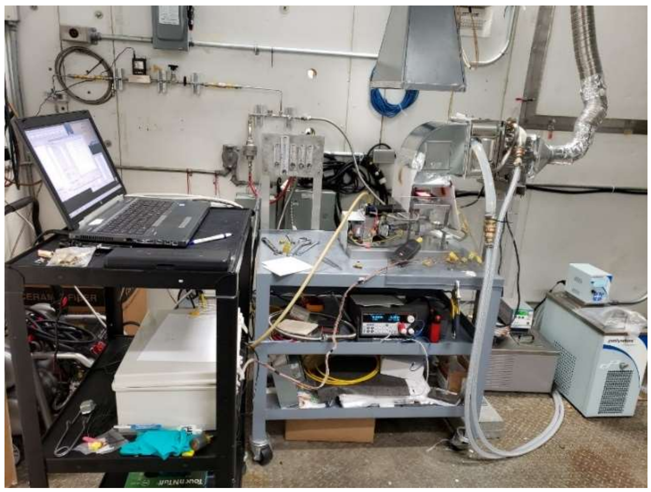

Figure 1. Hydrogen-blended NG burner test setup.

The flow range of a combined hydrogen blend can achieve 18,000 Btu/h with equivalence ratios up to 2. The K- and T-type thermocouples and IR temperature measurement (<1,300°C) capability have been added to track the thermal profile of the gas supply, hot surfaces, combustion module, and downstream products.

The heterogeneous burner design was finalized by incorporating features to enable uniform fuel distribution, thermal isolation, heterogeneous oxidation, low temperature catalytic oxidation, flame suppression, and reaction zone isolation. The burner head was designed to offer flexibility in accommodating the heterogeneous media. Burner media, sealing materials, and other necessary materials were incorporated.

1.2 PRELIMINARY EVALUATION

Different heterogeneous burner modules were subjected to preliminary evaluation for both baseline (with pure natural gas) and hydrogen-blend performance. Key test criteria to assess the safe performance included Btu/h rating, hydrogen concentration, burner surface area, and air-to-fuel stoichiometry. All burner modules were instrumented to establish the thermal profile of both hot combustion zone and cold feed supply and mixing zones to identify thermal lag, thermal runaway, and other combustion characteristics. Preliminary testing of a small-scale heterogeneous burner was performed at 3,000–4,000 Btu/h thermal rating using both natural gas and hydrogen blends, as shown in Figure 2.

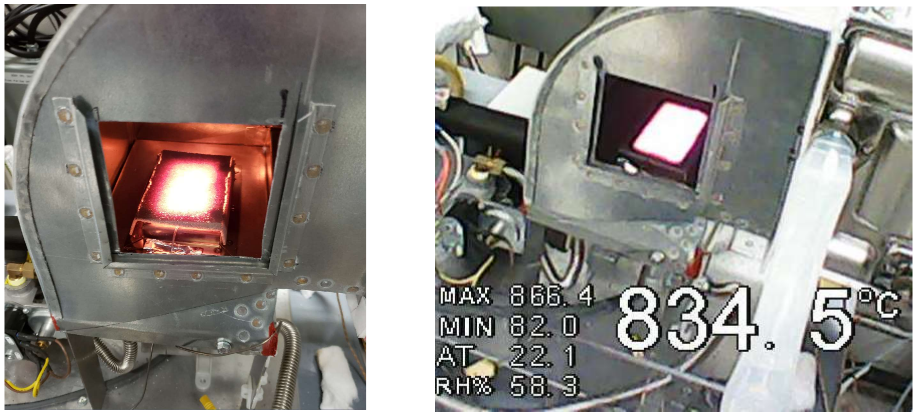

Figure 2. Preliminary evaluation of the 6 in.^{2} heterogeneous burner operating on 35% hydrogen-containing natural gas.

The feed supply and mixing zones did not exceed 40°C while the burner was operating at temperatures exceeding 800°C. These preliminary tests established the validity of the design approach undertaken to safely introduce hydrogen fuel in the feed mixture.

Burner heads with active surface areas in the range of 6 in.^{2} to 36 in.^{2} were evaluated in the test bay incorporated with gas control, instrumentation for flow and temperature measurement, data acquisition, and safety interlock. The experiments were initially conducted to evaluate natural gas performance at different thermal power ratings (Btu/h) by modulating the fuel flow rate. Once the safety and operability of the heterogeneous burner were established, the test was repeated by starting with natural gas and then gradually introducing hydrogen at different concentrations. This step was added to minimize the risk factor associated with hydrogen introduction in the fuel stream. The concentration and the overall fuel flow rate were varied on all burner configurations to establish a safe operating mechanism. The first set of tests was conducted by supplying fuel along with external air supply at 20% excess ratio (above combustion stoichiometry).

The key objective of these preliminary tests was to qualify all the burner configurations while integrated with the safety and operational aspects mentioned in section 1. Figure 3 displays the operational burners evaluated with a hydrogen-containing fuel mixture while supplied with stored compressed air at a desired stoichiometry for complete combustion.

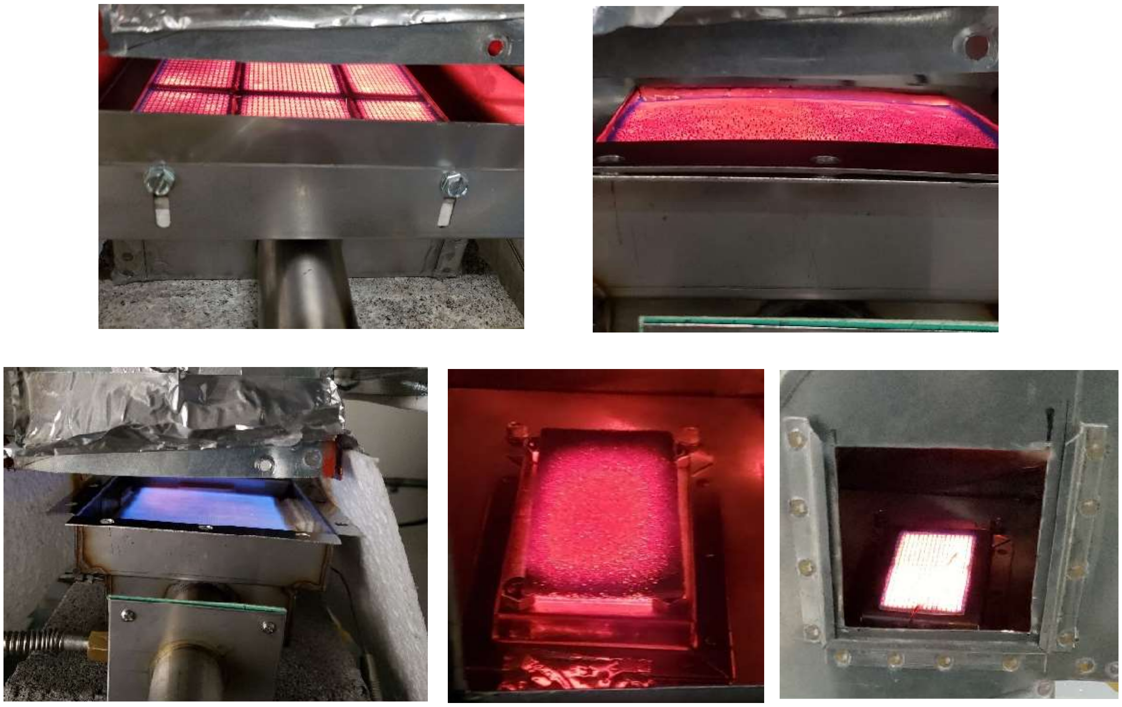

Figure 3. Flexible burner designs to accept different heterogeneous combustion media—premixed burner with external air supply.

1.3 FEED SUPPLY

The next step in the development of a prototype burner involved introduction of the feed mixture without imposing any parasitic energy burden, as would be expected from a conventional gas burner. Hence, optimization and evaluation of the feed, including combustion air stream to the blended gas burner, was investigated. Different air entrainment mechanisms (commercial off the shelf, COTS venturi nozzles) were evaluated to maximize the primary air supply ratio while using the secondary air feed at the combustion front initiated on the heterogeneous surface. Simultaneously, passive flow control through orifice sizing for delivering the necessary thermal power supply (Btu/h) to the burner was also optimized to identify precise orifice size for individual burners while utilizing the motive force offered by the gas supply at a pressure rating of 4.5 in. of water column (WC). Infrared output from burning the blended fuel mixture on the heterogeneous surface was successfully accomplished via a traditional orifice-based venturi nozzle. It was the only component in this design to include an orifice integrated with the heterogeneous burner, like the conventional flame-based burner design used in cooking ranges.

Based on this configuration, a detailed study was conducted to evaluate the heterogeneous burner performance under realistic operating conditions depicting cold start, ignition delay, hot restart, hydrogen concentration, thermal cycling, hydrogen-blend concentration influence on the startup, and others, to finalize the burner configuration.

1.4 DETAIL PERFORMANCE TESTING

A heterogenous burner with active surface area of approximately 36 in.^{2} was chosen for detailed performance evaluation (shown in Figure 4). This burner was selected to evaluate at the energy rating of 7,000–10,000 Btu/h.

The heterogeneous burner was supplied with variable amounts of fuel energy (Figure 5. The burner surface during operation with 10,200 Btu/h (left) and 6,400 Btu/h (right).) by modulating the fuel flow rate via inline restriction, at a steady hydrogen concentration of 30% in natural gas, as shown in Figure 4. The burner temperature was measured by a thermocouple located in the center and therefore may not be representative of the entire surface temperature.

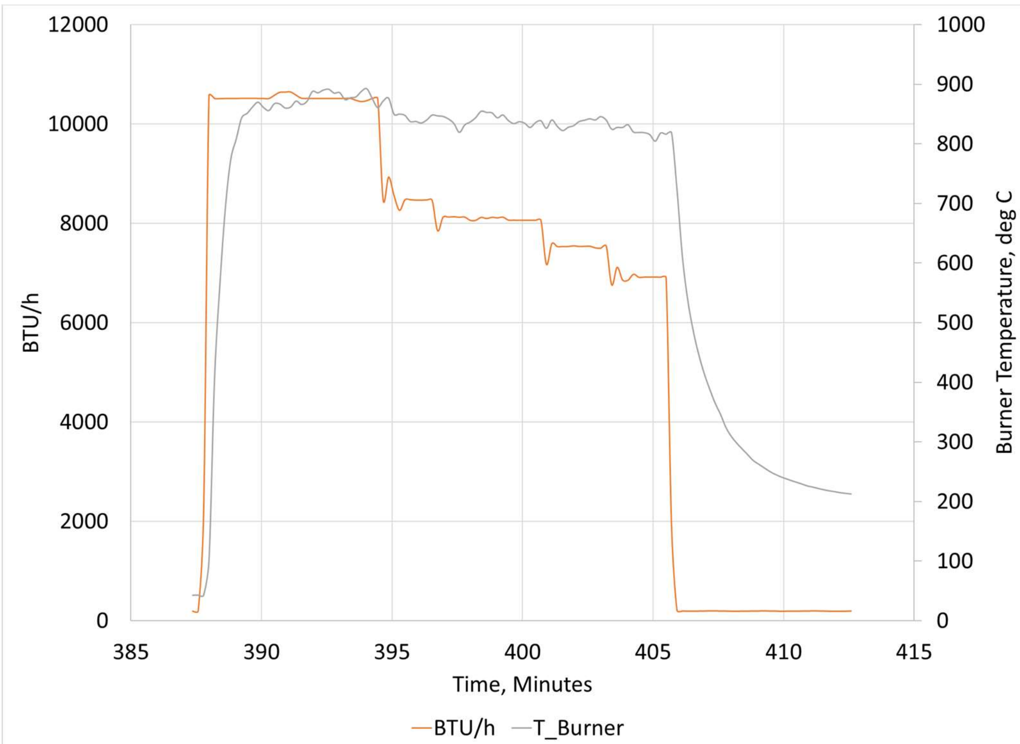

Figure 4. Heterogeneous burner temperature vs. fuel energy supply at 30% hydrogen concentration in natural gas.

Figure 5. The burner surface during operation with 10,200 Btu/h (left) and 6,400 Btu/h (right).

The heterogeneous burner was then evaluated for its performance at different hydrogen concentrations by slowly increasing the hydrogen flow rate after achieving steady state at each test point, as shown in Figure 6. Hydrogen was supplied from a regulated gas cylinder, whereas natural gas supply was from the pipeline, delivered to the burner at ~4.5 in. WC. Needle valves were employed to adjust the individual gas flow rates, monitored by mass flow meters. As shown, the burner temperature varied between 885°C and 830°C as the hydrogen concentration increased from 12% to 50% over the course of ~20 min. The differential pressure between the source gases led to a slight increase in the hydrogen concentration during the steady state operation and at shutdown. No flashback was observed during the entire test. This test establishes the flexibility of the burner in accepting a wide range of hydrogen concentrations.

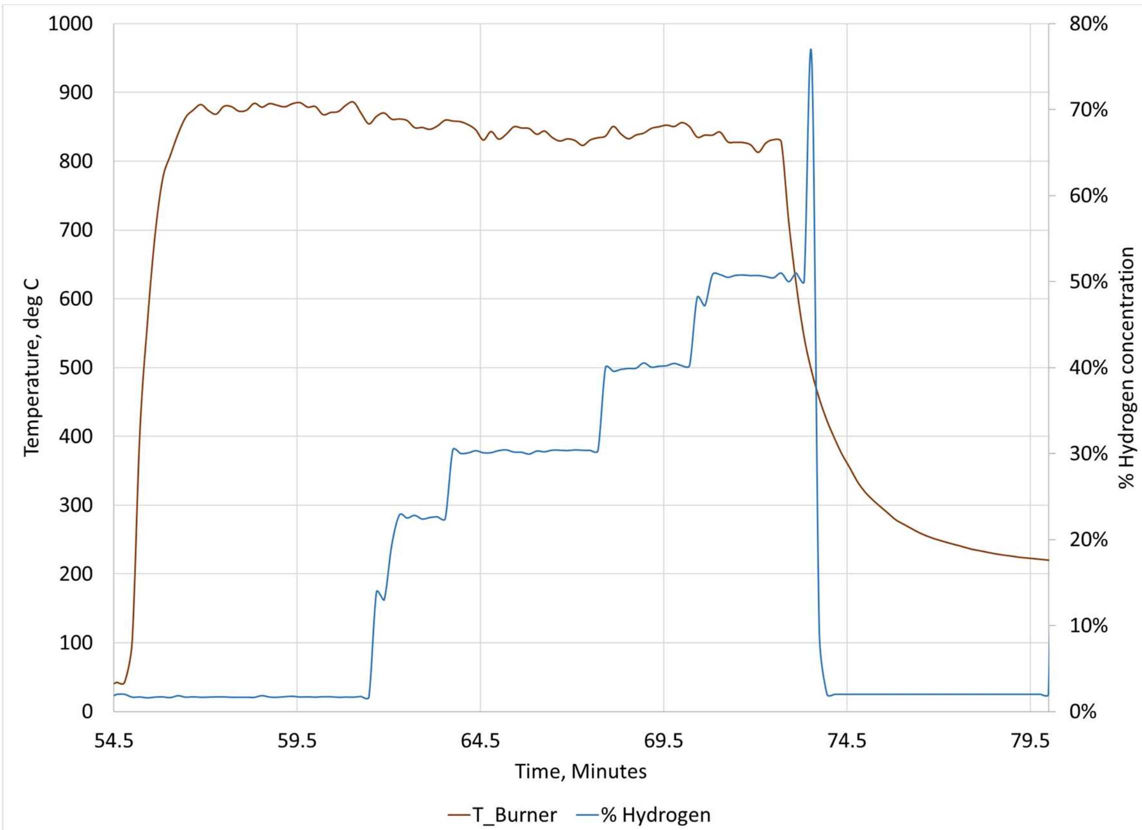

Figure 6. Heterogeneous burner surface temperature vs. hydrogen concentration.

Reliability of the burner was further evaluated by repeated cycling of the burner between on and off states via fuel shutoff, restart, and subsequent light-off to investigate the influence of surface temperature on flashback safety. This operating scenario is a key metric when considering desired level of safety expected from consumer appliances. Hence the heterogeneous burner was supplied with ~9,000 Btu/h of fuel containing 50% hydrogen blended with natural gas. Figure 7 displays the burner temperature and hydrogen concentration throughout the time tested. As shown, the burner achieves ~825°C while starting from different surface temperatures in the range of 180°C–560°C. Safe operation of the burner was observed without any signs of flashback during the 30 min test (Figure 8)

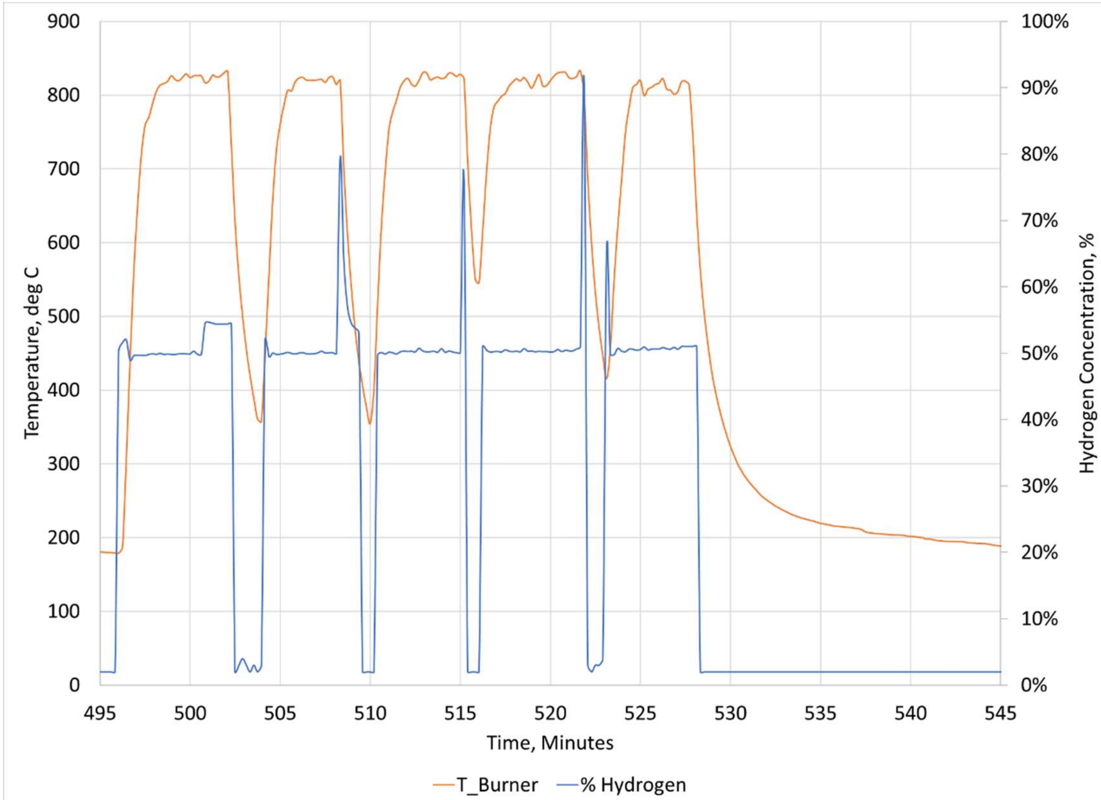

Figure 7. Thermal cycling test of the heterogeneous burner in the presence of 50% hydrogen. Also shown are the cold and hot restarts of the burner.

Figure 8. Heterogeneous burner operation with 50% hydrogen-blended natural gas. Thermal cycling and hot restart operating scenarios were tested.

Long-term evaluation of the heterogeneous burner (Figure 9) was also conducted to study the reliability of flashback safety during extended exposure to high concentrations of hydrogen and thermal conductance between the hot heterogeneous combustion surface and metal enclosure of the burner incorporated with combustion media and thermal isolation. The burner was operated for ~27 min, including a hot restart stage, at a rating of 8,000 Btu/h in the presence of 50% hydrogen concentration. The cold feed zone remained below 45°C during the entire test and showed no signs of thermal migration or flashback occurrence.

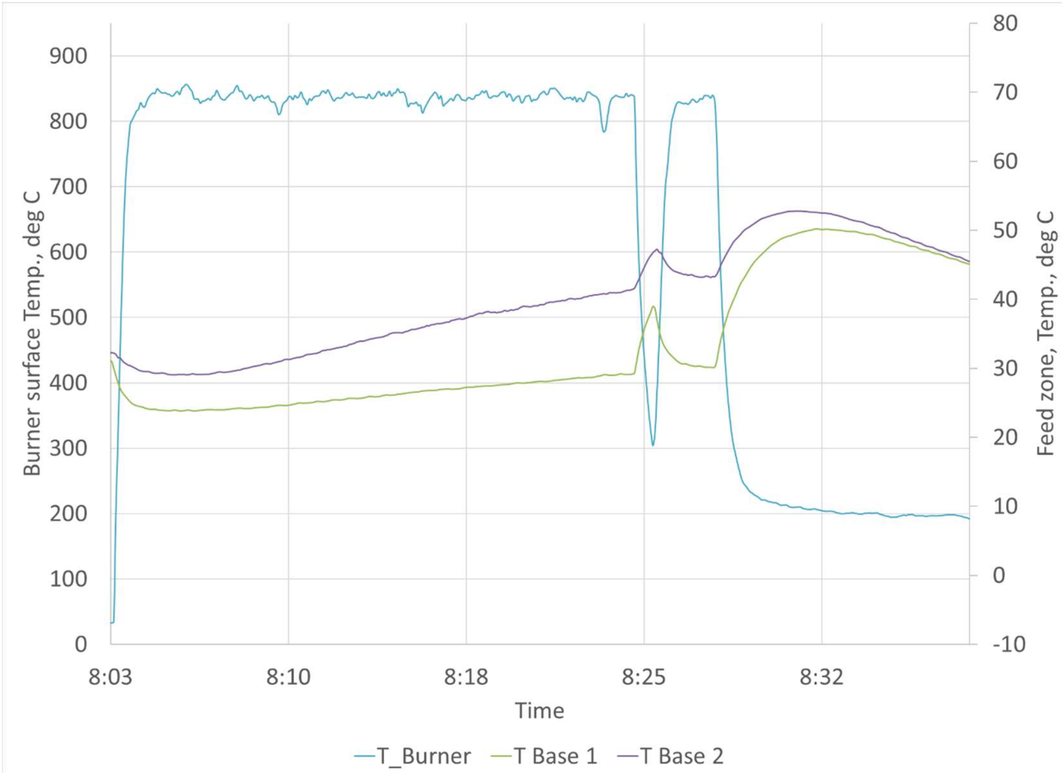

Figure 9. Long-term evaluation of the heterogeneous burner with 50% hydrogen, operated at 8,000 Btu/h rating.

2. PROTOTYPE APPLIANCE

2.1 EQUIPMENT MODIFICATION

A hydrogen fuel–compatible burner was designed, optimized, investigated, and reported on in the previous quarter. The main focus of the current milestone was to ensure that the developed hydrogen burner can be integrated with commercially available products. Requirements for integrating the developed burner in a commercially available cooking range were studied in the case of multiple commercial appliances—both recreational and residential models—as shown in Figure 10. Key requirements of startup, safety shutdown, and energy modulation were reviewed in both models.

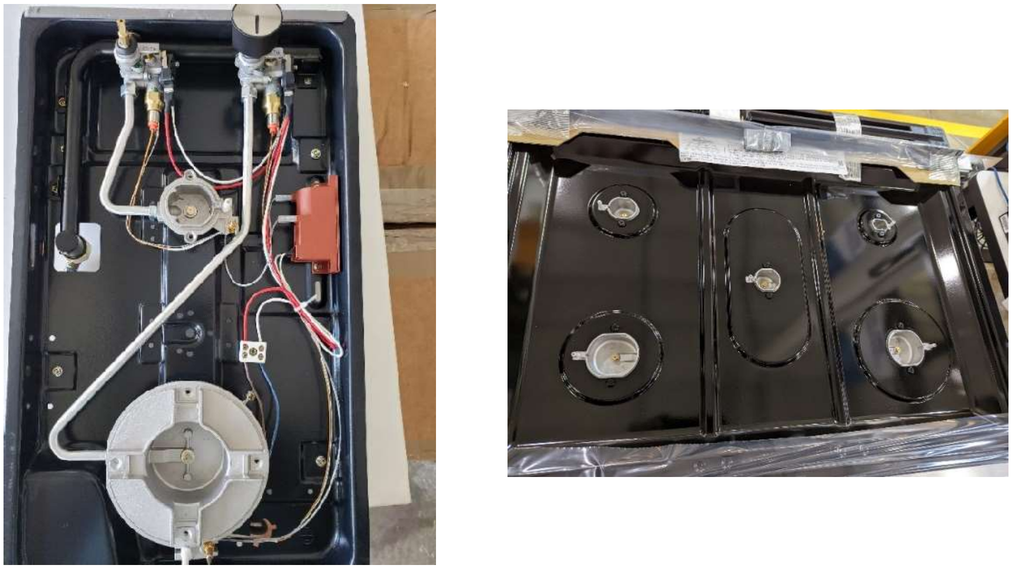

Figure 10. Traditional cooktops available to consumers.

Primary subcomponents in these models include fuel connection, fuel flow rate modulation, starter, thermal sensor, fuel shut-off valve, and a top plate to isolate system components from the hot zone. A majority of the residential models are not equipped with thermal sensors and fuel-shutoff valves, whereas models designed for compactness and fuel flexibility (such as the RV model) are generally integrated with secondary safety modules.

As shown in Figure 11, the thermal sense and spark electrode are mounted vertically in close proximity with the flame. Once a stable flame is established, the thermal sensor generates a voltage signal closing the fuel valve circuit. Depressing the fuel modulation valve makes a physical contact between the high voltage side of the transformer, which allows current to flow to the electrical ground (the cooktop's metal surface, where fuel is released through the open channels), which in turn generates a spark that momentarily initiates the ignition. The same mechanism is also employed in residential models, albeit without the thermal sensor and safety shutoff valve, as shown in Figure 12.

Figure 11. Cooktop equipped with thermal sense and spark electrode.

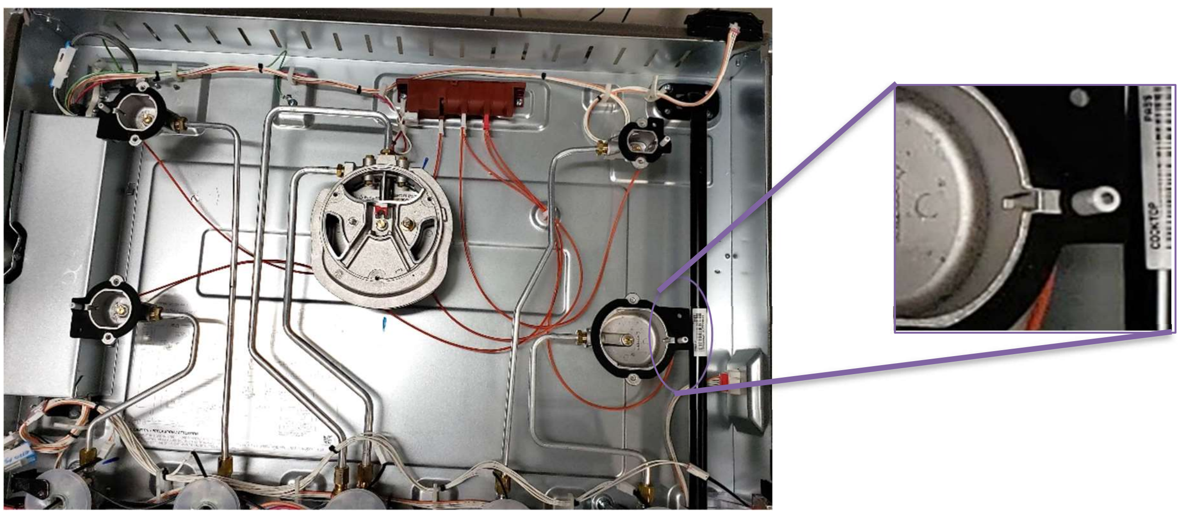

Figure 12. Residential cooktop equipped with the spark electrode.

Modification of the commercially available appliance was conducted to accommodate the developed burner for final integration with the starter, valve, and thermal sensing switch. The two-burner RV model was used for investigating the feasibility of integration and evaluating the performance. Key unit operations of thermal sense and spark ignition were physically integrated with the hydrogen burner module. Figure 13 shows the cooktop with the original flame-based burner suitable for natural gas/propane, whereas the heterogeneous surface oxidation burner suitable for hydrogen blends, natural gas and propane is shown in the top. The thermal sense module from the as-received cooktop was mounted on top of the heterogeneous burner so that the fuel shutoff switch is activated if the appliance detects no active heat generation. Similarly, the original spark module along with the transformer was deemed compatible with the new burner. Ground path for the spark module was accomplished by bolting the burner module to the sheet metal of the chamber.

Figure 13. RV/camping cooktop integrated with a hydrogen-compatible burner.

The initial prototype integrated with a hydrogen-compatible heterogeneous surface oxidation burner was subsequently evaluated for reliability and safety. As shown in Figure 14, the burner was tested with 50% hydrogen-blended natural gas fuel. The test was continued for ~20 min to ensure no thermal runaway in any of the sections of the burner installed inside the cooktop. Temperature measurements across all surfaces and critical zones of the feed supply and transition to the hot surface showed no influence of the containment of the burner inside the appliance, thereby demonstrating the viability of the integration approach.

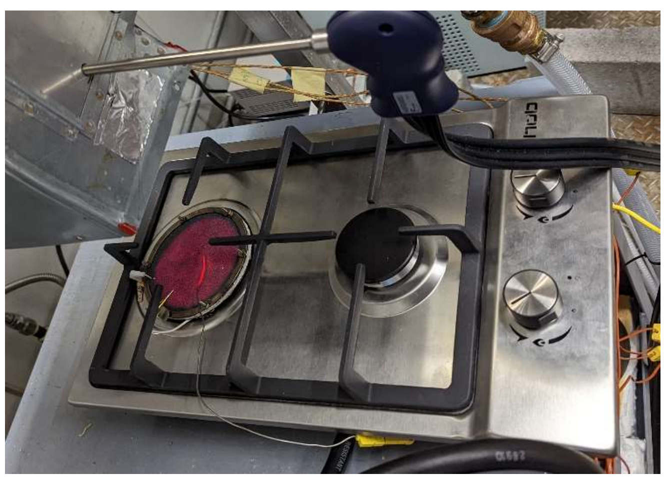

Figure 14. Preliminary evaluation of the hydrogen burner integrated in an RV cooktop appliance.

Similarly, the burner was evaluated by placing a solid metal plate on top of the burner to mimic the placement of a pot or pan. This test was conducted to evaluate the influence of a top surface and its proximity on primary and secondary air supply to the burner enabled by the venturi and hot gas buoyancy, respectively. No noticeable influence was observed during the startup/ignition phase and steady state operation. The test was then extended to a stainless steel pot filled with water, as shown in Figure 15.

Figure 15. Evaluation of the hydrogen-compatible cooktop with a cooking pot placed on the top.

Additionally, two different models of residential-scale cooktops were sourced and disassembled to evaluate the hydrogen burner integration feasibility. Top- and undermounted cooktop designs were acquired and investigated for the integration study, as shown in Figure 16.

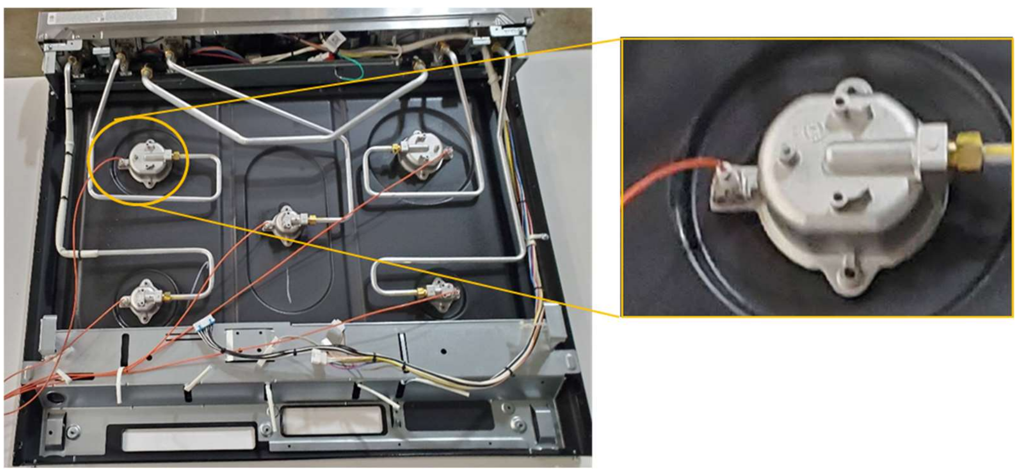

Figure 16. Residential cooktop with undermount burners and spark electrode.

Based on the successful integration and evaluation of the RV model, the residential design was modeled for integration with five burners compatible with hydrogen blends, as shown in Figure 17. The integration approach adopted for starter module mounting will be employed for the residential model, as well.

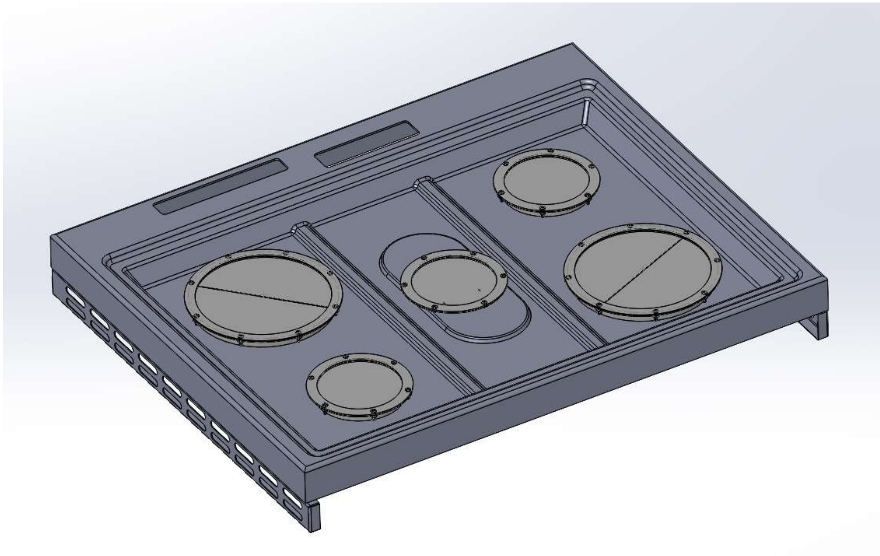

Figure 17. Computer-aided design model of a residential cooktop integrated with hydrogen-blend fuel–compatible burners.

2.2 PERFORMANCE EVALUATION

The prototype cooktop was used for evaluation at a wide range of hydrogen concentrations. Figure 18 displays the burner head temperature, Btu/h rating of the burner, and hydrogen concentration as a function of time.

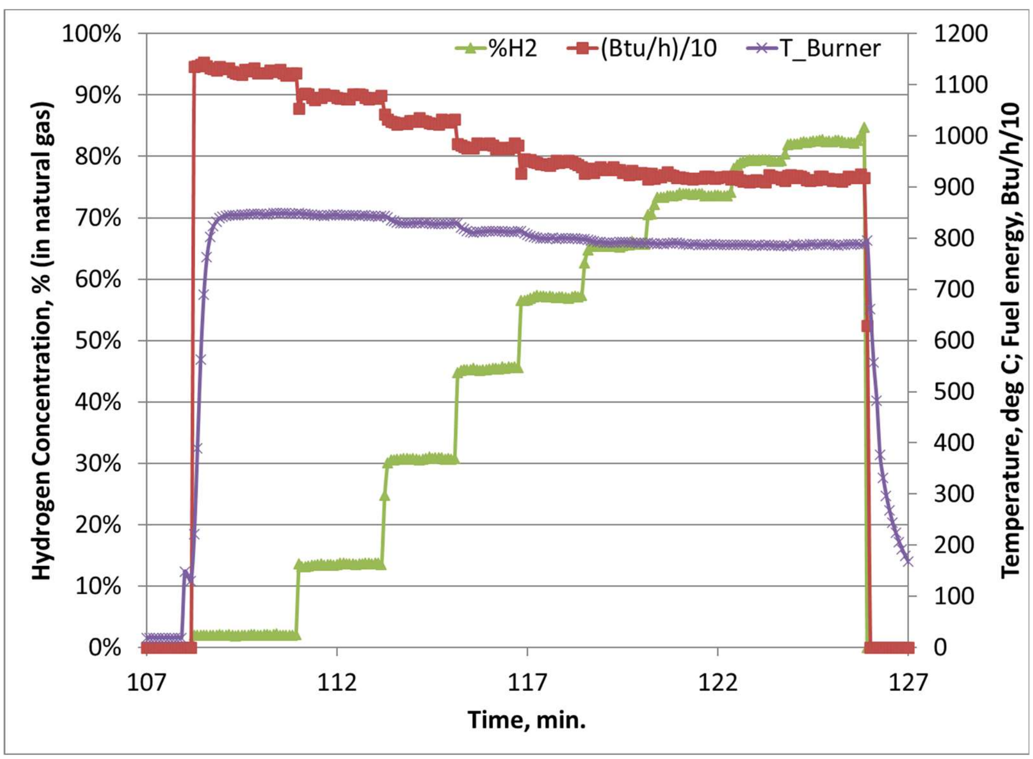

Figure 18. Hydrogen-blend performance of the prototype appliance.

As shown, the hydrogen concentration was increased from 0% to 82% while the surface temperature and the total amount of energy supplied were measured. It can be seen that the surface temperature stayed around 800°C during the course of the test but was flexible in accepting a broad range of hydrogen concentrations.

Thermal efficiency tests were also conducted on the prototype appliance. Thermal efficiency of the developed burner was compared with that of the traditional burner by operating individual burners at identical operating conditions. In this test, 600 g of tap water was collected in a 300 series food-grade, cooking-quality stainless steel pot (NSF 79020/ANSI 2) measuring 8 in. tall and 4.5 in. in diameter. The initial temperature of the water was ~21°C. Because the traditional burner is incompatible with hydrogen blends, the efficiency test was conducted on natural gas on both burners. Temperature of the water was measured at precisely 1 in. below the water level and 1.5 in. away from the container wall to avoid the influence of ambient heat loss on the measured value by securing the thermocouple in a hole drilled through the lid of the container, as shown in Figure 19. Fuel flow rate and temperature measurements were logged. Water temperature was monitored during the test and allowed to reach at least 100.5°C before the fuel supply to the burner was switched off. The boiling test was performed at two different flow rates of 1.4 SLPM and 2.4 SLPM.

Figure 19. Experimental test setup to investigate energy efficiency improvement with the prototype appliance.

Figure 20 shows the time to reach the desired boiling temperature when the traditional burner and the hydrogen-compatible burner are operated at identical conditions. As can be seen at 2.4 SLPM natural gas fuel flow rate, the traditional burner takes ~9 min, whereas the hydrogen burner takes ~8.5 min. However, at a lower flow rate of 1.4 SLPM, the hydrogen burner takes ~10.5 min, whereas the traditional burner takes ~12 min. Efficient utilization of fuel can be seen with the hydrogen burner owing to infrared heat energy produced, particularly at lower flow rates. Further tests will be conducted at a wide range of fuel flow rate values.

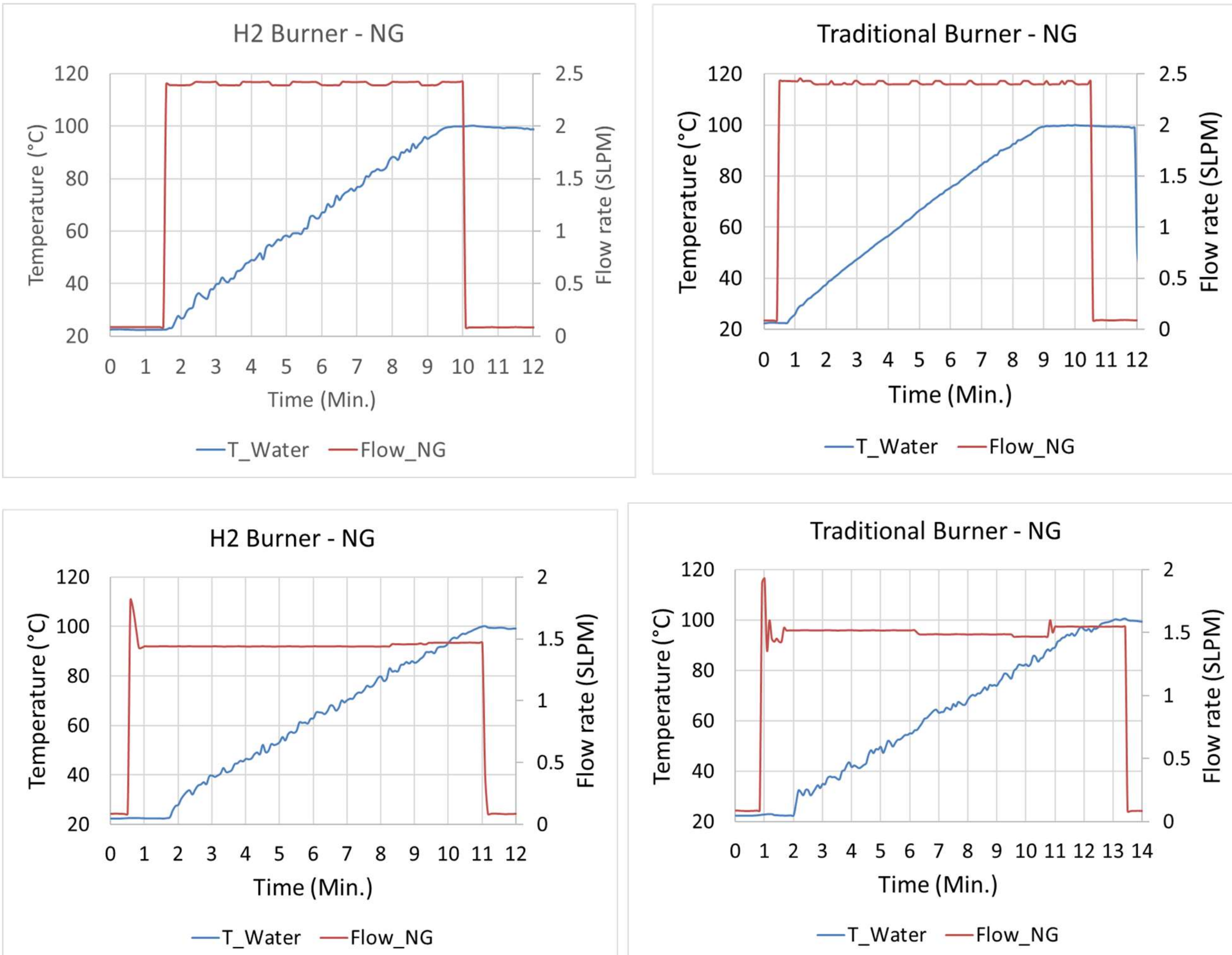

Figure 20. Measured temperature of water as a function of time at 2.4 SLPM and 1.4 SLPM fuel flow rate with a traditional flame burner and a hydrogen-compatible burner.

The influence of container size on heat transfer efficiency was investigated by repeating the tests with a larger pot measuring 6.5 in. diameter while also varying the total amount of thermal load by increasing the amount of cold water in a food-grade stainless steel 300 series container, as shown in Figure 21.

Figure 21. Tests using a food-grade stainless steel 300 series pot with a 6.5 in. diameter.

The temperature of the water was measured at precisely 0.5–1 in. below the water level and 1.5 in. away from the container wall to avoid the influence of ambient heat loss on the measured value. Fuel flow rate and temperature measurements were logged. Water temperature was monitored during the test and was allowed to reach ~75°C before the fuel supply to the burner was switched off. The boiling test was performed at a fixed fuel flow rate of 2.4 SLPM for total water content of 700 g. Figure 22 shows the time to reach the desired boiling temperature while operated at identical conditions with the traditional burner and the hydrogen-compatible burner. Cumulative fuel consumption was calculated from the measured flow rate values on two burners operating at different conditions. As shown, at 2.4 SLPM fuel flow rate and 700 grams of water the traditional burner consumed 16.45 liters of fuel while the hydrogen burner consumed ~13.3 liters, yielding approximately 20% increase in energy efficiency. Analysis of the results presented earlier show that the total fuel supply was decreased from 15.5% – 17.5% with the 4 in. diameter pot operated at 2.4 and 1.4 SLPM flow rates, demonstrating the improved energy efficiency with the hydrogen-compatible infrared burner.

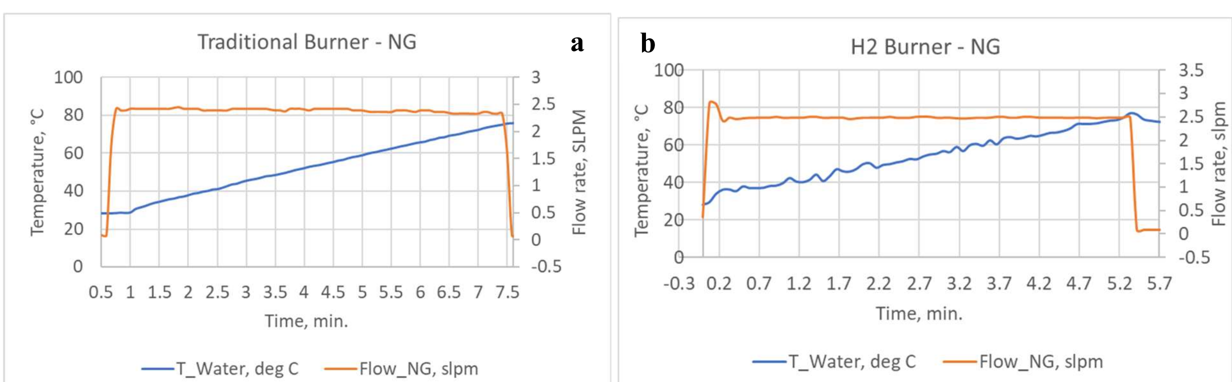

Figure 22. Measured temperature of water as a function of time at 2.4 SLPM fuel flow rate and 700g of water, with a traditional flame burner and the hydrogen-compatible burner.

3. RESIDENTIAL COOKING RANGE

3.1 EXPERIMENTAL SETUP

Feed gas was prepared by mixing precisely calculated flow rates of hydrogen, pipe natural gas, and air streams using a combination of mass flow controllers (MKS Instruments), and rotameter flow meters. The delivery pressure was controlled and monitored (<6 in. WC) via needle valves and pressure transducers, respectively. K-type thermocouples were used for measuring temperatures across the fuel supply and combustion sections of the burner. Test data were logged using a Campbell Scientific data logger (model CR1000). For some of the tests, certified premixed gas containing 46% methane, 2% ethane, and 52% hydrogen was directly supplied (Airgas) by modulating with a needle valve and tracked by mass flow meter (Omega FMA1600 series). Nitrogen oxide (NO_x), hydrocarbon, carbon monoxide, carbon dioxide, and oxygen emissions were measured with Sauermann SICA-230 & 4500-2 emission analyzers.

NO_x emissions (nanograms/joule) were calculated based on higher heating value calorific correction, according to Equation (1)[1,2]. In the equation, $CO_{2,msd}$ represents the measured carbon dioxide concentration in the combustion gases (%), $CO_{2,bkg}$ represents the ambient carbon dioxide concentration (0.05%), Mi represents the molecular weight of the species considered (30 for NO), and $molCO_2/MJFuel$ is the number of moles of carbon dioxide generated by combusting all carbon sources (methane and ethane), expressed as a function of total higher heating value (HHV) of all hydrocarbons consumed in the combustion process. HHV of methane was assumed to be 55.5 MJ/kg, and HHV of ethane was assumed to be 51.9 MJ/kg.

$$C_i\left(\frac{ng}{J}\right) = \frac{0.1 * C_{i,ppm}}{(CO_{2,msd,\%} - CO_{2,bkg,\%})} * \left[\frac{molCO_2}{MJ\ Fuel}\right] * M_i\left(\frac{g}{mol}\right). \tag{1}$$

Carbon monoxide and hydrocarbon concentrations were corrected for air-free values using Equation (2)[1,2], where $C_{i,msd}$ is the measured concentration of the pollutant, $C_{i,bkg}$ is the background concentration of the same molecule, and $O_{2,msd}$ is the concentration of oxygen (%) in the combustion product stream.

$$C_i(@0\%\ O_2) = \left(C_{i,msd} - C_{i,bkg}\right) * \left[\frac{20.95}{(20.95 - O_{2,msd,\%})}\right]. \tag{2}$$

3.2 TEST RESULTS

The cooking range with upgraded burners was installed in a new test facility (Figure 23) to operate at a combined capacity of ~30 kBtu/h and with the capability of accepting different concentrations of hydrogen in the range of 0%–90%. The test facility included a dedicated multispeed ventilation system and safety mechanisms involving excess flow shut off valve, gas sensing, alarm system, and data acquisition. This ensured safe evaluation of the hydrogen-compatible cooking range at different operating scenarios such as hot restart, cold start, energy modulation, surface temperature variance, flow rate, and operational time.

---

[1] Singer, B. C., Apte, M. G., Black, D. R., Hotchi, T., Lucas, D., Lunden, M. M., and Sullivan, D. P. (2009). *Natural gas variability in California: Environmental impacts and device performance experimental evaluation of pollutant emissions from residential appliances*. No. LBNL-2897E. Lawrence Berkeley National Laboratory, Berkeley, CA.

[2] Zhao, Y., McDonell, V., and Samuelsen, S. (2019). "Influence of hydrogen addition to pipeline natural gas on the combustion performance of a cooktop burner." *International Journal of Hydrogen Energy*, 44(23), 12239–12253.

Figure 23. Cooktop test facility equipped with ventilation, safety interlocks, and variable feed supply.

The assembled cooking prototype was commissioned and evaluated for complete performance including overall functionality, safety, emissions, and energy utilization efficiency. The cooktop was operated on both natural gas and 50% hydrogen-containing gas simultaneously to deliver ~35,000 Btu/h of energy, as shown in Figure 24. The cooktop was designed to accept either natural gas or hydrogen-blended natural gas with four burners, whereas a dedicated conventional blue flame natural gas burner was also incorporated for comparative studies.

Figure 24. A hydrogen cooktop operating with 50% hydrogen-blended natural gas.

The cooktop was operated with natural gas blended with hydrogen fuel at wide range of concentrations (Figure 25). As shown, the minimum Btu rating of the burner was preserved at a value of >10,000 Btu/h, whereas the hydrogen concentration in the blend was increased from 0%–60% without any modification to the feed supply because the entire test was conducted in a single test in an atmospheric burner with a fixed orifice.

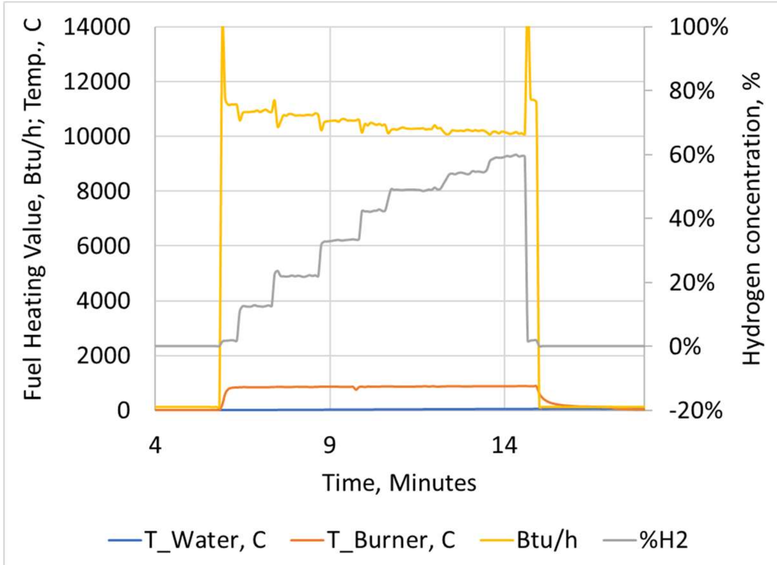

Figure 25. Fuel flexibility of the heterogeneous oxidation infrared burner operating at different concentrations of hydrogen.

The test was repeated on a smaller burner with a maximum capacity of 4,000 Btu/h. The hydrogen concentration was increased from 0% to 80%, as shown in Figure 26. The total delivered thermal energy remained above 4 kBtu/h irrespective of the fuel mixture supplied. Additionally, the reliability of the burner was also examined by introducing flow perturbance at high concentrations of hydrogen beyond 80%. The burner temperature remained stable despite the broad fuel composition and delivered energy content. The surface combustion ensured complete combustion in a reliable manner without triggering any safety concerns. Both burners delivered temperatures in the range of 800°C–900°C.

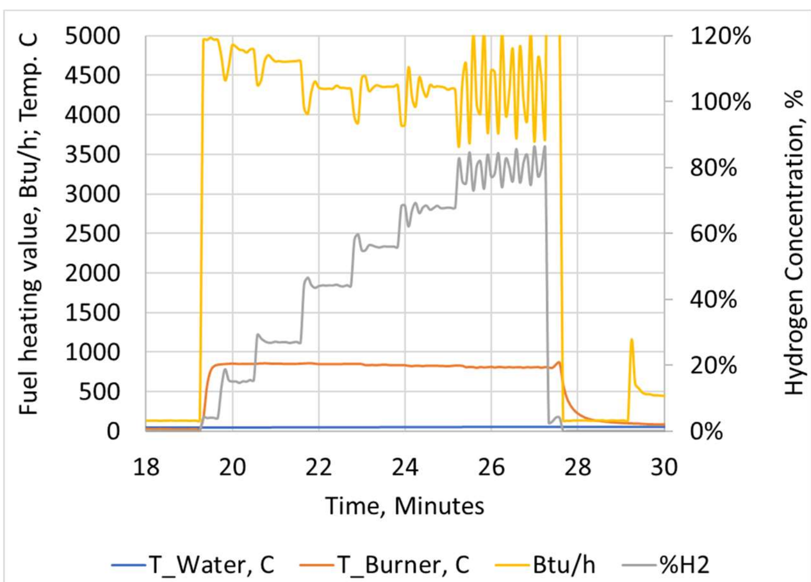

Figure 26. Fuel flexibility, reliability, and robustness validation of the heterogeneous oxidation infrared burner operating with induced flow perturbance.

Switching to 100% hydrogen fuel in the heterogeneous oxidation IR burner described above showed fuel leakage at the venturi when using pressures of ~4–5 in. WC embedded with a smaller porosity media

(0.6 mm diameter compared with 1 mm diameter pore with blended fuel). However, the leak disappeared when the fuel pressure was increased to values >12 in. WC and the burner operated as expected, as shown in Figure 27. The leak was caused by the higher pressure drop across the combustion media. This issue was eventually addressed by removing the venturi and adding a dedicated air supply line, resulting in a premixed burner operating with pure hydrogen and air at a stoichiometry of 1.3.

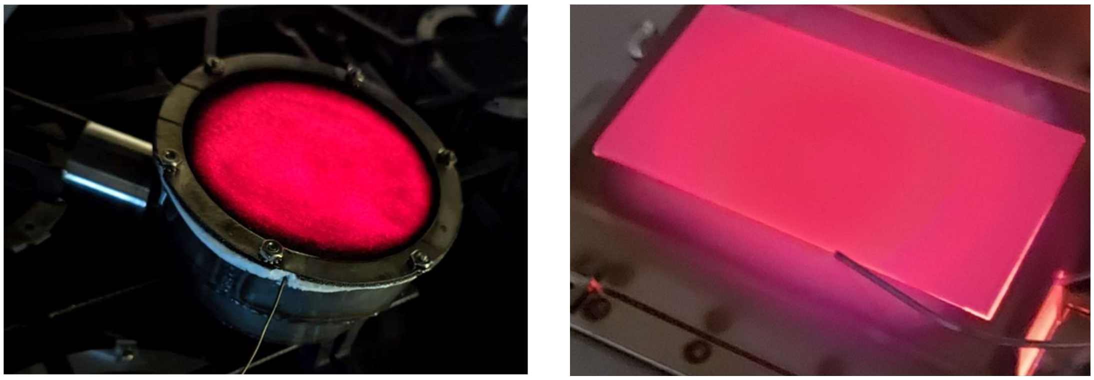

Figure 27. Operation of the heterogeneous oxidation burner with 100% hydrogen in (left) an atmospheric burner and (right) a premixed burner.

However, it should be noted that the cooking range burners are typically air-breathing, atmospheric burners where a venturi supplies primary air in addition to the fuel owing to entrainment of ambient air through the venturi. As stated previously, the fuel pressure plays a critical role in a leak-free, reliable performance when the developed heterogeneous oxidation burner is used. The premixed design showed risk-free operation when 100% hydrogen stream is used, as shown in Figure 27.

NO_x emissions were also measured from the hydrogen-compatible infrared burner with those of a conventional blue flame burner. Figure 28 displays the emissions measured at ~6 in. from the hot surface. The IR burner showed no measurable NO_x emissions, whereas the conventional blue flame burner exhibited NO_x emissions at >10 ppm. The equivalent calorific corrected value (lower heating value–based) was <1 ng/J for the IR burner, whereas the conventional blue flame burner emitted ~24 ng/J. Also, the lower NO_x emitting advantage of the IR burner was maintained throughout the cold start and sustained combustion time periods. Similarly, emissions from the IR burner stayed below 2 ng/J when supplied with various concentrations of hydrogen blended with natural gas. Figure 28B displays the NO_x emission measurements taken during the experiment reported in Figure 25. As shown, the measured CO_2 concentration (right axis) is lower than the values displayed in Figure 28 owing to the presence of lower carbon content associated with natural gas caused by higher hydrogen dilution. Similarly, the air-free concentrations of carbon monoxide remained in the range of 20–30 ppm in the case of a conventional burner and 40–160 ppm in the case of an IR burner (lower for higher hydrogen concentrations). No measurable CH_4 emissions were detected during these tests.

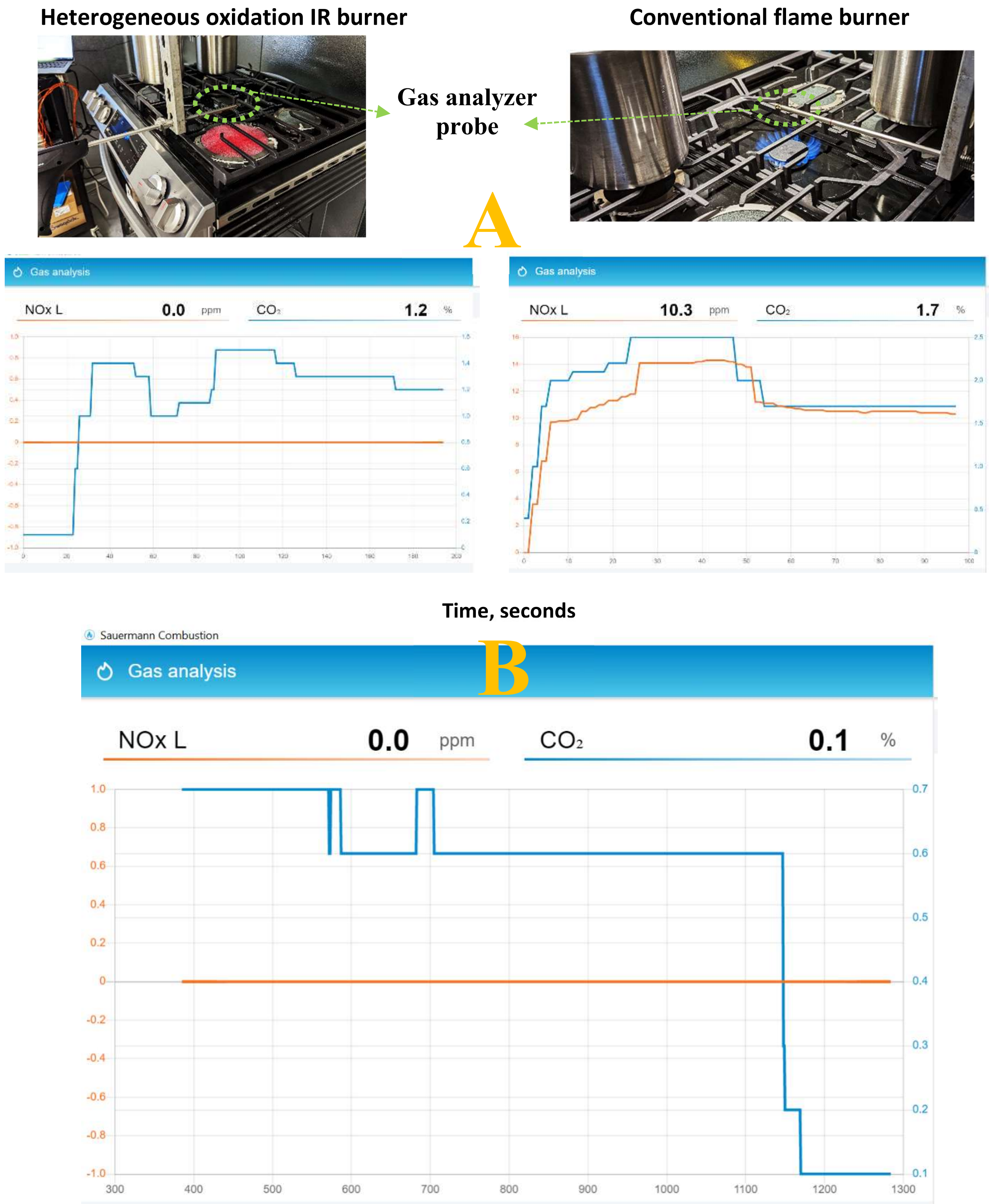

Figure 28. (A) NO_x emissions from conventional burner vs. hydrogen-blend that fueled Oak Ridge National Laboratory's (ORNL's) infrared burner; (B) NO_x emissions measured during the hydrogen-blend concentration study shown in Figure 25. The ORNL burner is pictured at top left, and the conventional burner is pictured at top right.

Another advantage of the developed IR burner is its energy utilization efficiency. Hence, thermal efficiency of the developed burner was compared with that of the traditional burner by operating individual burners at identical operating conditions. For the study, 6,000 g of tap water were collected in a 300 series food-grade, cooking-quality stainless steel pot (NSF 79020/ANSI 2) measuring 12 in. tall and 12 in. diameter. The initial temperature of the water was ~20°C. Because the traditional burner is incompatible with hydrogen blends, the efficiency test was conducted on natural gas on both burners. Temperature of the water was measured at precisely 1 in. below the water level and 1.5 in. away from the container wall to avoid the influence of ambient heat loss on the measured value by securing the thermocouple in a hole drilled through the lid of the container, as shown in Figure 29. Fuel flow rate and temperature measurements were logged. Water temperature was monitored during the test and allowed to reach at least 50.5°C before the fuel supply to the burner was switched off. The boiling test was performed at a nominal flow rate of 5.5 SLPM on the conventional burner and 5.2 SLPM on the IR burner. Figure 29 shows the time for the traditional burner and the hydrogen-compatible burner to reach the desired temperature while operated at identical conditions. The traditional burner consumed ~55 standard liters of natural gas over the course of ~10 min, whereas the IR burner consumed ~47 standard liters over the course of ~9 min. Compared with the conventional blue flame burner, the infrared burner lowered the total energy consumed by ~15% owing to efficient heat transfer from the infrared surface via simultaneous radiant and convective heating, as shown in Figure 29.

Thermal cycling capability and safety of the burners integrated in the cooking range were also tested. Figure 30 shows the thermal cycling safety of the two capacity burners supplied with 50% hydrogen-blended natural gas. The small burner was subjected to 15 cycles. The first 10 cycles allowed the hot surface temperature to reach below 100°C before restarting, whereas the last 5 cycles occurred at higher temperatures in the range of 200°C–680°C. Similarly, the large burner was also operated for seven cycles with the first three at a lower restart temperature, followed by the last four at higher restart temperatures, as shown in Figure 30.

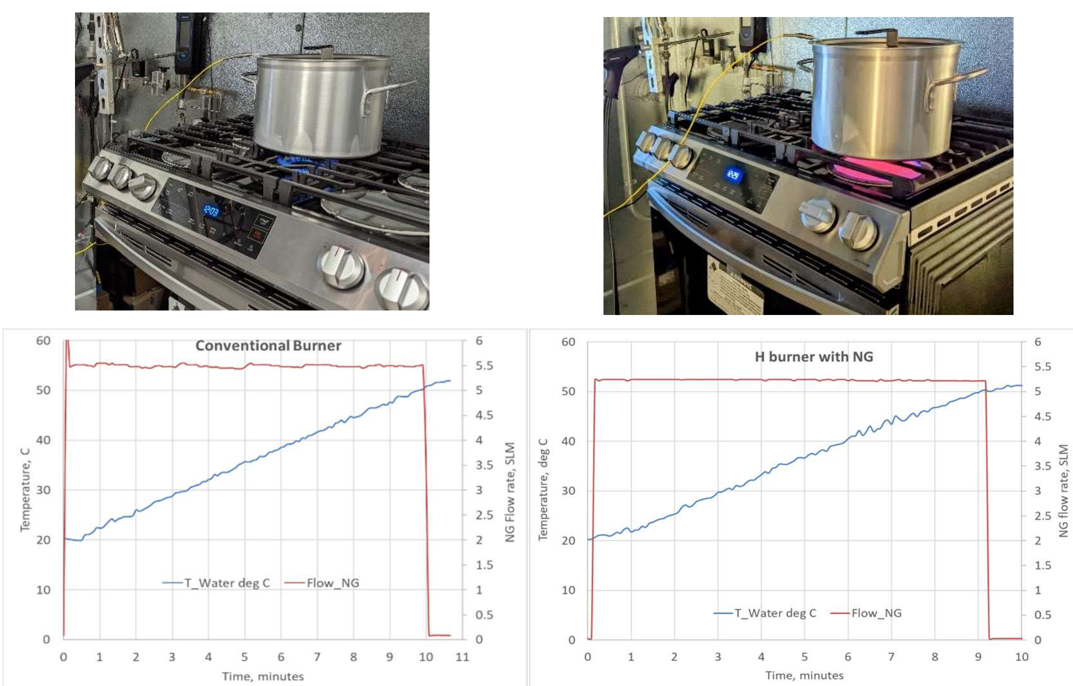

Figure 29. Energy efficiency tests of the (left) conventional burner vs. (right) ORNL's fuel-flexible burner. The top row shows photos of the pots with water temperature sensors, and the bottom row shows comparison charts for the tests.

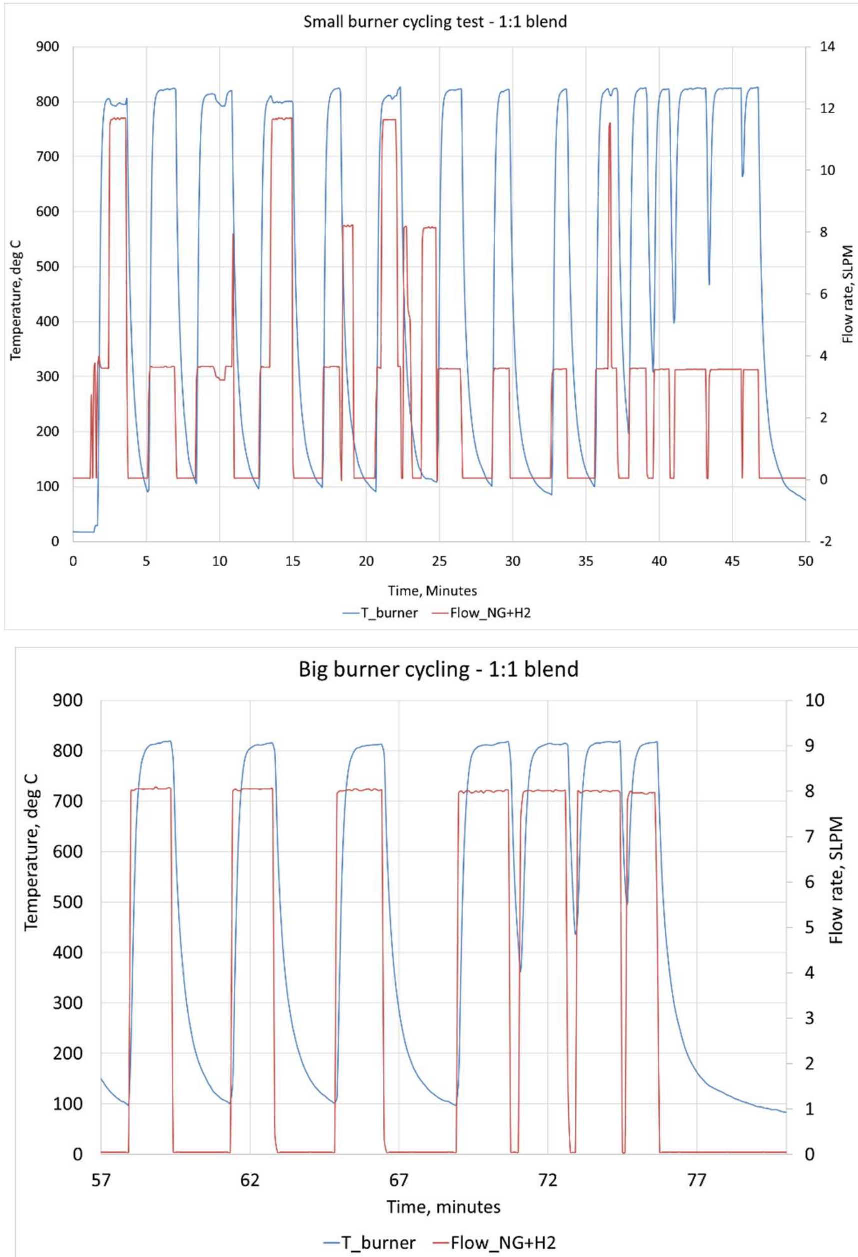

Figure 30. Thermal cycling and start-stop cycling of the two burners in the cooking range, operated with 50% hydrogen-blended natural gas.

An oven burner was designed after measuring the available space and cavity within the oven compartment. All the critical dimensions and features were considered and maintained to ensure air entrainment during operation for both primary (at the venturi) and secondary (inside the enclosure). The atmospheric burner works by entraining air from the cavity underneath the cooking range. Air is naturally entrained from both the back and bottom panels where openings are provided to pull in fresh air for combustion owing to buoyancy of hot gases.

The oven cavity was modified to accommodate the designed burner while ensuring unrestricted air flow and supply to the burner. The oven burner was then integrated with the oven cavity/chamber along with controls, sensing, and startup hardware, as shown in Figure 31. The hot surface igniter was integrated with the frame and tied to the original system controls. The overall air entrainment pathway and exhaust ventilation pathway were preserved in the design approach undertaken. Similar to the original burner, the updated hydrogen-compatible burner was enclosed underneath the spill tray where the combustion products vent from the opening on both sides of the tray and enter the oven cavity. We will evaluate this burner in the next reporting period.

Figure 31. Installation of the integrated oven assembly in the cooking oven.

The oven burner was supplied with 50% hydrogen-blended natural gas fuel and successfully operated, as shown in Figure 32.

Figure 32. Hydrogen-blend–fueled oven burner.

The measured emissions from the oven burner were still much below the values generally noticed from conventional flame-based burners. Figure 33 shows the measured NO_x emissions during the test using the 50% blend concentration. The equivalent value with calorific correction is ~1.5 ng/J, compared with >20 ng/J noticed from flame burners.

Figure 33. NO_x emissions from the hydrogen-blend–fueled infrared oven burner.

4. TECHNO-ECONOMIC ANALYSIS

4.1 MARKET ASSESSMENT

Gas cooking equipment is essential in the food processing and food service industry. It is basic equipment for cooking, roasting, and similar food preparation tasks in residential and commercial kitchens. Food service, hospitality, and household sectors have fueled the demand for gas burners used in kitchens. Manufacturers of gas ranges are focused on producing high-quality appliances with new technology and the latest designs. These factors are expected to drive the demand for gas ranges in the global market. Commercial gas stoves' market share, size, business revenue, future growth, trends, top key players, and business opportunities have been analyzed and forecasted until 2028[3]. A sample report has been sourced for the North American market.

Across the US, more than 33% of residential and commercial buildings use natural gas for cooking, representing an energy burden of 1,735 trillion Btu and emitting 97 million metric tons of annual carbon dioxide emissions. Additionally, secondary air pollutants such as methane, carbon monoxide, and NO_x are co-emitted and released indoors, which can trigger respiratory diseases. A recent study showed NO_x measurements averaged 21.8 ng/J, comprising 7.8 ng of NO_2 per joule and 14.0 ng of NO per joule[4]. Kitchens lacking range hoods and having poor ventilation have been shown to easily surpass the national standard of 100 ppb/h of NO_2 accumulation. As a result, stringent regulations are being enforced to achieve clean combustion in gas equipment. For instance, the latest Air Quality Management Plan standards state a limit of 5–8 ng/J for majority of building equipment, including furnaces and water heaters. Residential and commercial cooking equipment emission standards are also being developed to contain NO_x emissions.

4.1.1 Technical Challenges

Conventional flame-based burners lead to high NO_x emissions owing to the extreme adiabatic flame temperature[5]. Presence of hydrogen in hydrocarbon-based fuel such as natural gas further increases the

[3] https://www.marketwatch.com/press-release/commercial-gas-stoves-market-share-size-2022-business-revenue-future-growth-trends-top-key-players-business-opportunities-forecast-to-2028-2022-06-08.
[4] Lebel, E. D., Finnegan, C. J., Ouyang, Z., and Jackson, R. B. (2022). "Methane and NO_x Emissions from Natural Gas Stoves, Cooktops, and Ovens in Residential Homes." *Environmental Science & Technology*, 56(4), 2529–2539.
[5] Dimopoulos, P., Bach, C., Soltic, P., and Boulouchos, K. (2008). "Hydrogen–natural gas blends fuelling passenger car engines: combustion, emissions and well-to-wheels assessment." *International Journal of Hydrogen Energy*, 33(23), 7224–7236.

adiabatic flame temperature, resulting in undesired emissions[6]. The high flame velocity of a hydrogen-enriched natural gas burner also makes it susceptible to flashback, thus creating a significant safety hazard. Recent studies[7] have clearly established the risk of flashback at hydrogen concentrations starting at 20%. Flame stability is another challenge associated with broad variations in fuel composition. Substitution of natural gas with zero carbon fuels may entail only minor combustion system modifications if the burner is capable of avoiding some of the known issues—such as flashback, emissions, flame visibility and stability, high temperature and reactivity. In view of these challenges, scientific work was undertaken to design a fuel-flexible combustion module to accept hydrogen and its blends with natural gas while improving combustion stability and heat transfer efficiency and offering significantly lower NO_x emissions. To overcome these challenges, ORNL designed a hydrogen-compatible hybrid infrared-convective flameless burner that relies on heterogeneous catalytic oxidation of the fuel mixture. A hybrid combustion module integrating a novel heterogeneous combustion surface with tailored thermal and fluid transfer characteristics enabled safe, clean operation of the burner at moderate temperatures. Using this approach, the energy of combustion is distributed via IR over a much larger surface and, therefore, at a lower temperature. As a result, NO_x emissions are significantly reduced (measured at <2 ng/J) because the combustion occurs at a nominal temperature of 900°C–1,100°C, compared with 1,500°C in traditional flame-based burners where the propensity for thermally induced NO_x formation is much higher. The IR energy from the burner is ideally suited for cooking appliances because the heat transfer efficiency is higher compared with the convective mechanism. Additionally, the heterogeneous burner is fuel flexible because it can accept the readily available natural gas as well as blends of green hydrogen and natural gas. The prototype appliance (see the full technical report) has been shown to accept a wide range of hydrogen compositions without posing safety concerns.

4.2 COST ANALYSIS

Given the efficiency, emissions advantages, and hydrogen compatibility of the heterogeneous oxidation burner, a cost analysis was conducted to evaluate the economic viability of the burner. The developed design consists primarily of heterogeneous media, a metal housing including venturi, fuel distribution plenum, and insulation. Quotations for different quantities were acquired from all corresponding vendors. Figure 34 shows the projected cost of the burner (12,000 Btu/h thermal rating) at quantities ranging from 100 to 100,000.

As can be seen, the cost of manufacturing such a burner varies from $10 to $46. The economy of scale diminishes beyond quantities exceeding 10,000. Figure 35 shows the cost distribution for the same burner; the media is the most expensive part in the design, followed by metal housing and welding/assembly costs.

The retail price of a similar thermal rating conventional flame burner was found to be ~$56. A profit margin of 60% projects the potential cost of manufacturing the die-cast aluminum burner head at ~$22.50. The projected cost of the developed heterogeneous burner is comparatively similar at a production quantity of 1,000 units.

[6] Maznoy, A., Pichugin, N., Yakovlev, I., Fursenko, R., Petrov, D., and Shy, S. S. (2021). "Fuel interchangeability for lean premixed combustion in cylindrical radiant burner operated in the internal combustion mode." *Applied Thermal Engineering*, 186, 115997.
[7] Zhao, Y., McDonell, V., and Samuelsen, S. (2020). "Assessment of the combustion performance of a room furnace operating on pipeline natural gas mixed with simulated biogas or hydrogen." *International Journal of Hydrogen Energy*, 45(19), 11368–11379.

Figure 34. Cost projection of the developed burner as a function of production volume, based on sales quotes for parts and labor.

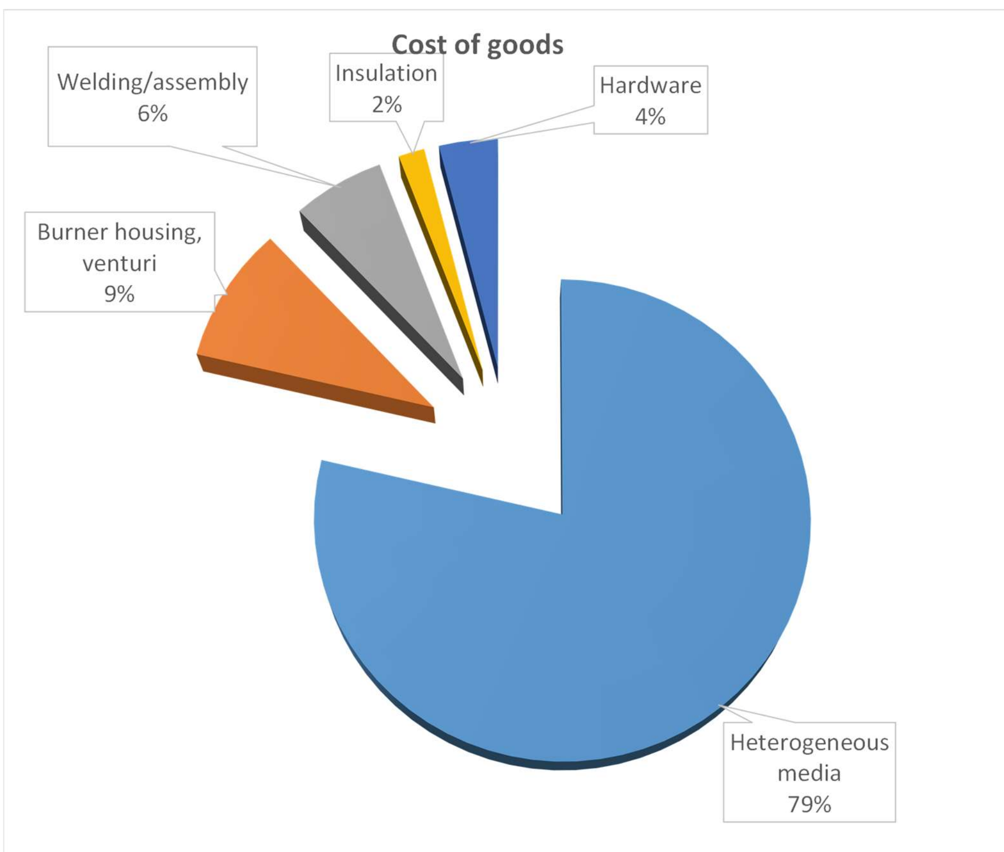

Figure 35. Cost distribution for the developed burner.

5. SUMMARY

A novel hydrogen-compatible heterogeneous burner prototype was engineered, fabricated, and evaluated for applications in cooking appliances. The key features targeted and accomplished under this effort included fuel flexibility, tolerance to high hydrogen concentrations (up to 85% in atmospheric design and 100% in premixed design), a wide range of thermal power ratings, thermal cycling, reliability, and most importantly, safety. The burner was operated in the range of 3,000–12,000 Btu/h under all practical operating conditions (cold start, hot restart, fuel concentration variance). The heterogeneous oxidation burner technology was evaluated for overall performance targeting safety, reliability, emissions, fuel flexibility, and energy efficiency in commercial RV and residential cooking range appliance prototypes. The burner demonstrated safe, reliable performance generating infrared heating energy without the consumption of any parasitic energy while using low-cost materials. Performance evaluation testing of the novel IR burner demonstrated fuel flexibility with hydrogen-blended natural gas while significantly eliminating air pollutants like NO_x and methane and increasing the energy efficiency by up to 20%.